A.C. FIELD MEASUREMENTS: A NEW METHOD FOR DETECTING AND MEASURING FATIGUE CRACKS

W.D. Dover, F.D.W. Charlesworth, K.A. Taylor,

Mechanical Engineering Department, University College London, London, U.K.

ABSTRACT

Recent advances in the theory and practice of A.C. Field measurements have made it possible to produce a new N.D.T. instrument capable of detecting and sizing surface cracks in any metal. This paper describes the basic electronics, and established operational procedures used with this instrument and discusses several commonly met electrical field distributions. The use of the instrument is illustrated by measurements on part-circular notches and cracks in a steel elongator roll and a tubular welded joint.

KEYWORDS

N.D.T.; A.C. crack measurements; part-circular cracks; crack detection.

INTRODUCTION

The concept of structural integrity through fail safe procedures has recently become more widely adopted and this has led to new inspection problems. The earlier use of this design philosophy concentrated on thin section structures where the failure was preceded by the presence of a crack extending entirely through the thickness. This type of crack is normally visible in service or laboratory tests so that understanding of crack growth behaviour can be established and inspection procedures set up without too much difficulty.

More recently it has become desirable to adopt similar procedures for components and structures made from thick sections. The implementation of fail safe procedures for these structures is substantially different as fatigue cracks initiate and grow as surface cracks in thick sections and may cause fracture prior to reaching the through-the-thickness condition. The behaviour of these surface cracks has to be studied in the laboratory and they must be measured in terms of length and depth in service. Appropriate inspection procedures can be set up once this information is obtained. Unfortunately existing inspection techniques have, so far, proved to be inadequate for this purpose, even for the laboratory work. This has led to the situation where there is insufficient information on surface crack growth behaviour for designers. Faced with the problem of obtaining crack growth data from thick section structural models, in our own work, it was decided to attempt to develop a new inspection system for this purpose. The instrument described in this paper is the result of those efforts (1)(2). This instrument is now commercially available (3)(4).

A.C. FIELD MEASUREMENTS

The potential drop method has been used previously with both D.C. and A.C. for measuring cracks. However, only A.C. is likely to be useful for large structures. Most previous users employed some form of calibration so that the measured voltage could be interpreted in terms of crack size. This approach proved to be cumbersome and innacurate and consequently led to the technique being little used. Two problems held up the further development of this technique. Firstly, it was not possible to explore the electrical field on the surface of a component or structure in terms of the true surface voltage. The measured values contained a pick-up error which was variable. This error affected the repeatability of the voltage readings. Secondly, even if the true surface voltage could be measured few theoretical solutions were available for the electrical field distribution. These two problems have now been overcome so that it is now possible to combine the experimental surface field measurements with a theoretical solution to give estimates of crack shape without any need to calibrate.

The theoretical field distribution should always be determined for any new cracked specimen geometry but fortunately one simple solution, the uniform field, is valid for many geometries. The uniform field situation is used in the following in order to illustrate the general approach to A.C. Field Measurements.

Consider a semi-infinite metal solid as shown in Fig. 1. If an a.c. input is applied to the surface an electrical field will exist as shown. The main feature of this field is that the current is carried in a thin layer at the surface; this is known as the 'skin effect'. The theoretical analysis of a plane wave in a good conductor shows that the skin depth, δ, can be defined as follows:

$$\delta = \frac{1}{\sqrt{\mu_r \mu_o \pi \ \sigma \ f}} \qquad (1)$$

where

δ = Skin depth, m

μ_r = Relative permeability of conductor

μ_o = Permeability of free space

= $4\pi \times 10^{-7}$ H/m

σ = Conductivity, S/m

f = Frequency of a.c. source, Hz.

For a material such as mild steel, a frequency of 5K Hz would give a skin depth of about 0.13 mm.

Returning to Fig. 1. it can be seen that for a semi-infinite solid the portion of the field bounded by EFDC can be considered as uniform, i.e. a probe with fixed contact separation distance (Δ) would record the same voltage irrespective of location provided that the contacts were aligned parallel to AB. The crack faces would also give the same probe voltage if it were physically possible to measure on these faces. It is important to note here that this would not be true if the crack reduced the cross-section by more than a few percent. The assumption of a

uniform field would then become invalid.

If the field is uniform the crack depth can be estimated by placing the probe on the line AB, but not bridging the crack, and recording the probe voltage V_1. The probe is then positioned on AB so that it spans the crack and a second voltage V_2 is recorded. For V_1 the path length between the contact points is Δ. For V_2 the path length is Δ + 2d, where d is the crack depth. As the field is uniform it is possible to combine the two readings as follows:

$$\frac{V_1}{\Delta} = \frac{V_2}{\Delta + 2d}$$

This can be rearranged to give the following:

$$d = (V_2/V_1 - 1)\,\frac{\Delta}{2} \qquad (2)$$

Equation 2 will be referred to as the one-dimensional solution and will be used as the basis for other two-dimensional cases.

This simple procedure can now be used because it is possible to measure the true surface voltage accurately and repeatably. The electronic systems required to achieve this accuracy will now be briefly described.

A block diagram of the electronic system is shown in Fig. 2, and the equipment is shown in use in Fig. 3. The instrument consists of two distinct parts; the current source, used to set up the a.c. field, and a sensitive a.c. voltmeter to measure the field voltage. These are combined into one case, the voltmeter being located at the front and the current source at the rear.

The drive oscillator uses a thermistor stabilised Wien bridge circuit which provides good amplitude and frequency stability. The output from this oscillator is fed into a constant-current power amplifier which drives the current through the test specimen. The connections to the specimen are not critical and magnets, screw connections, clamps etc have been successfully used. The impedance of the current loop can vary quite widely for different applications but for an a.c. frequency of 5 KHz a range of from zero to three ohms is typical. The input to the voltmeter i.e. the field voltage measured by the probe, is frequently very small and could be less than a microvolt. However there are occasions when the voltage can be much higher, depending on specimen material and geometry. To achieve the required high sensitivity and resolution the voltmeter must be designed for very good noise performance. This implies a narrow bandwidth and in the present case this has been achieved by use of a synchronous rectifier circuit. So that one can achieve good linearity and stability this rectifier is at the end of the measurement chain. To prevent overloading of the amplifier by any interference some additional filtering is required at the input and this is achieved with an active filter (5) arrangement based on the Wien bridge circuit. This choice promotes close matching and tracking of oscillator and filter.

Applications

This technique has been used successfully on many thick section applications in service including steam chests, turbine casings, threaded connections, welded steel joints etc (2). Some of these applications are described here to illustrate the use of the system.

The first application concerns the measurement of cracks in thick section tubular welded joint. This work is part of a laboratory programme aimed at supplying fatigue data for Offshore Structures. The programme has followed two approaches providing stress-life data and fatigue crack growth data. For the latter, extensive crack measurements have been taken to ascertain the crack shape and crack growth rates for a variety of geometries and load cases. Figure 4 shows some of the data from this programme measured on a T-joint tested under out-of-plane bending. The measurements were made with a hand held probe (Δ = 10 mm) with input contacts located about 100 mm either side of the weld. Most of the cracks have been chord cracks located at the weld toe. The growth of these cracks, although starting from the weld toe, is predominantly in the parent metal. Consequently the initial voltage reading V_1, was always taken on the parent metal at a site very close to the weld toe.

Figure 4 shows how the crack shape generally developed in these intermediate life tests. Several semi-elliptical cracks form at adjacent sites around the weld toe and eventually join up to give one major crack. This work is more fully described elsewhere (6) but it can be seen that very detailed information on crack shape can be recorded.

One example, sometimes met, is where the crack has an aspect ratio of less than ten. For these cracks the field is not uniform and equation 2 cannot be used to provide an accurate value of the crack depth profile. The theoretical solution for this field has been developed however (2) for cracks of different shape i.e. part-circular, semi-elliptical, triangular, square etc. These solutions are presented in the form of a multiplier to be applied to a depth estimate using equation 2.

Consider the results shown in Fig. 5 which are for a part-circular surface notch of size 38 x 10.4 mm located in a mild steel plate. A set of voltage readings were taken at various sites along the crack for the probe adjacent (V_1) to and spanning (V_2) the crack. The disturbance of the electrical field due to the crack is $\frac{V_2 - V_1}{V_1}$ and this can be calculated from theory and compared to these experimental results. Figure 5 shows the variation of $\frac{V_2 - V_1}{V_1}$ with distance from the crack centre-line (x) where the crack half length is a. As can be seen the agreement between theory and experiment is good; the error at the centre-line being of the order of 10%. It is of interest to note that the electrical field is disturbed at points beyond the end of the crack and that the experimental measurements confirm the behaviour. This could be utilised in situations where the crack is hidden, under a rivet head for example.

The data shown in Fig. 5 can also be interpreted in terms of crack size. The simplest approach would be to use equation 2. This would introduce an error because the analysis which led to equation 2 assumed a uniform field which is not true for the part-circular crack. Figure 6 shows the interpretation of the experimental data of Fig. 5, in terms of crack size using equation 2. It can be seen that although this interpretation gives a reasonable answer for many situations, an underestimate of 44%, there are circumstances where a closer estimate is desirable. The true interpretation of the data shown in Fig. 5, using the theoretical field distribution, is also shown in Fig. 6. This time the error between the estimated size and the real size is smaller, 8% and acceptable for most purposes.

This example highlights several important aspects of the use of A.C.F.M. for crack measurement. Although many situations exist where the uniform field solution forms a reasonable approach the field should always be explored using the probe to check the validity of this assumption. In addition, if the crack is an irregular shape the field measurements around the crack can give additional information which can be used to assess the crack shape. It can be seen from this example that the

system has been perfected to the stage where theory and experiment agree. This has led to the possibility of a much wider range of applications than was previously considered possible.

A further application illustrates the effect of gross changes in section size due to the crack. This example was prompted by some measurements of crack depth using A.C.F.M. on a steel elongator roll (7) which was subsequently taken out of service because of the findings and sectioned to determine the actual crack depth. The two sets of results are displayed in Fig. 7 and show good agreement. The estimated crack sizes, using equation 2, slightly overestimate the real depth, unlike the results of Fig. 6. This discrepancy suggested that the field could be varying on the crack faces due to the substantially reduced section size at the crack location. An experiment was conducted to test this theory using a cylindrical steel bar possessing a circumferential groove. In addition, the electrical field on the groove face was analysed theoretically and it was found that the voltage readings V_1 and V_2 should be interpreted using the following equation:

$$d/r_o = 1 - \exp\left\{ - \frac{\Delta}{2r_o}\left[\frac{V_2}{V_1} - 1 - \frac{hd}{\Delta(r_o - d)}\right]\right\} \qquad (3)$$

Figure 8 shows the voltage readings interpreted using both equations 2 and 3. It can be seen that the uniform field assumption leads to a very large overestimate of crack depth, when the crack is deep, but the proper interpretation using equation 3 gives a value which is within 10% for all sizes. For the practical example of the elongator roll the crack sizes were such that the error using equation 2 was acceptable. However the example shows that the field must be interpreted properly at all times just in case the error in applying equation 2 is unacceptable. The previous example was one where the field could be checked with the probe. In this example considerable changes in section size at the crack location led to electrical field irregularities. Both possibilities should be checked in a new application.

CONCLUSIONS

(1) A new crack measurement system has been produced capable of accurately sizing surface cracks in large structures. This technique does not require any calibration prior to use.

(2) Examples of crack measurement in welded joints, cylindrical components and low aspect ratio notches have been described. The error in these measurements was generally better than 10%

REFERENCES

(1) Dover, W.D., Charlesworth, F.D.W., Taylor, K.A., Collins, R. and Michael, D.H. Symp. on Eddy Current Characterisation of Materials and Structures. N.B.S. Washington, Sept. 1979.

(2) Dover, W.D., Charlesworth, F.D.W., Taylor, K.A., Collins, R. and Michael, D.H. "A.C. Field Measurements: Theory and Practice."

(3) The Unit Inspection Co., Sketty Hall, Swansea, SA2 8QE.

(4) Instron Ltd., Coronation Road, High Wycombe, Bucks., HP12 3SY.

(5) Williams, P. "Band Pass filters using Wien's Bridge". Electronic Letters, Vol. 6, No. 6, March 1970, pp 186-187.

(6) Private Communication, British Steel Corporation, Tubes Division.

(7) Dover, W.D. and Holdbrook, S.J. "Fatigue crack growth in tubular, welded connections" BOSS 79, London (Imperial College), August 1979, paper 40.

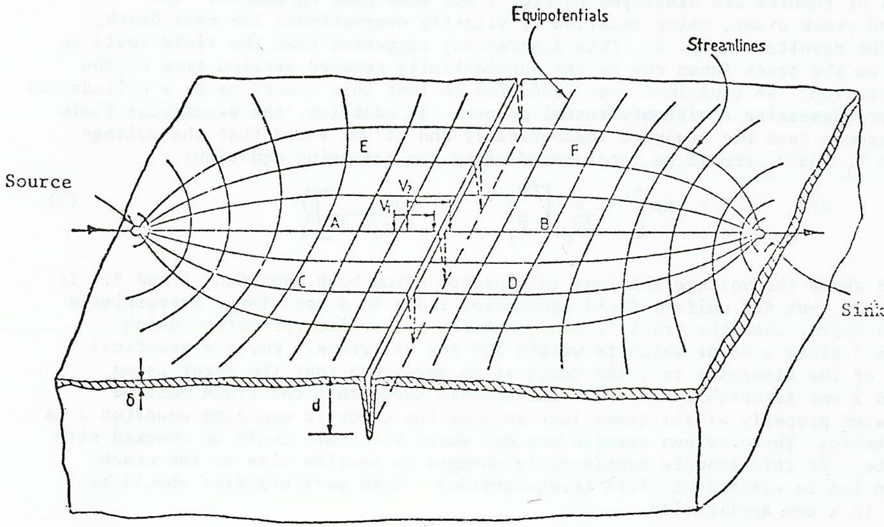

Fig 1. A.C. field in a semi-infinite solid possessing an infinitely long edge crack.

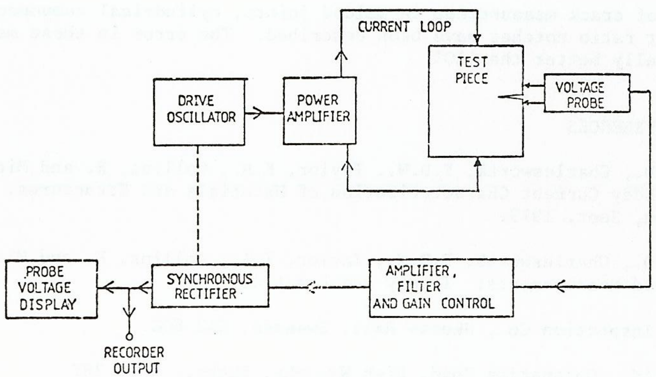

Fig 2. Block diagram of the Crack Microgauge electronic system.

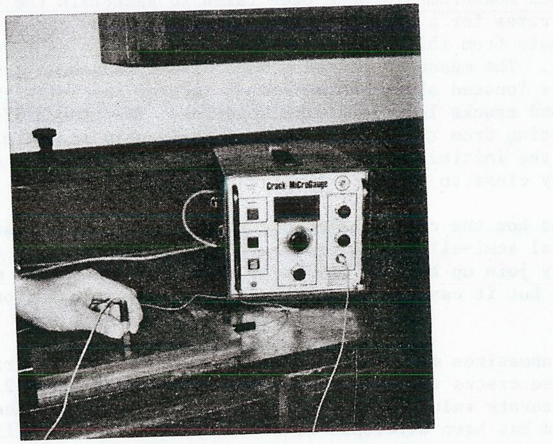

Fig 3. Crack Microgauge in vee for measuring a surface crack.

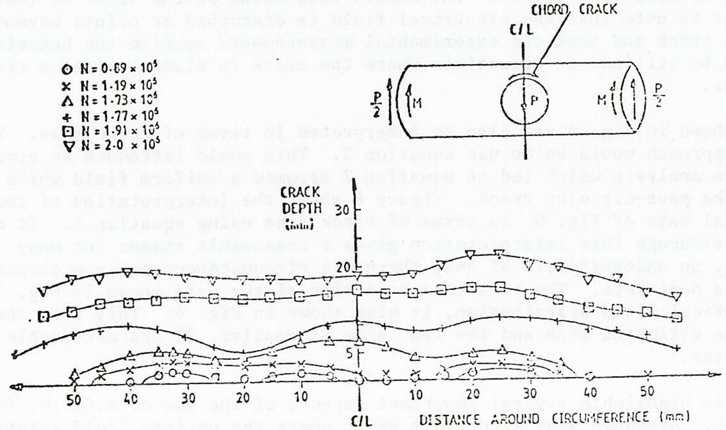

Fig 4. Crack shape development recorded during a random load fatigue test on a T-joint.

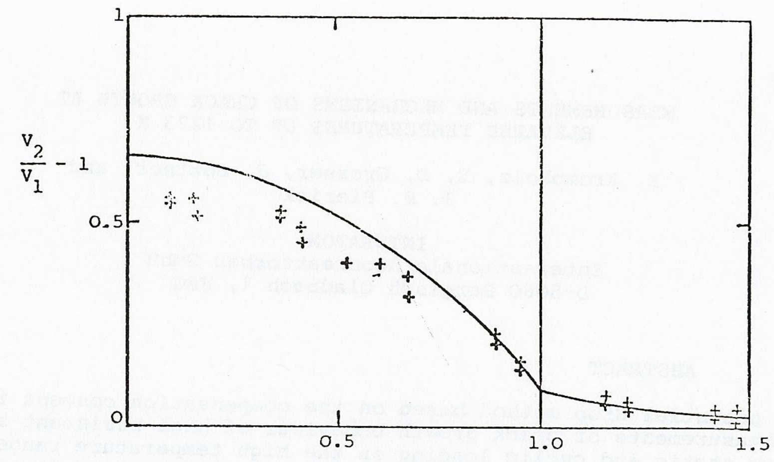

Fig 5. Distribution of A.C. field along the crack.
Ref. 2. + Experimental results.

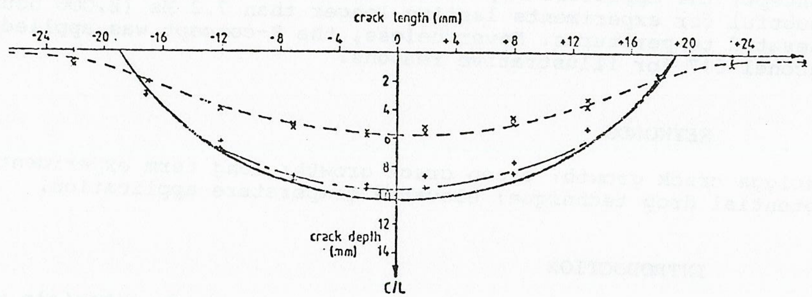

Fig 6. Part circular notch sized using the Crack Microgauge ---- Eq.2 (one-dimensional) —— —— Ref.2 (two-dimensional) - ——— Actual shape.

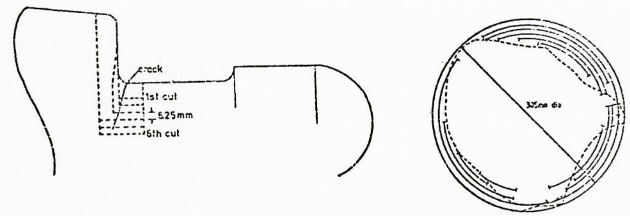

Fig 7. Fatigue crack measurements using A.C.F.M.
optical - - - Crack Microgauge.

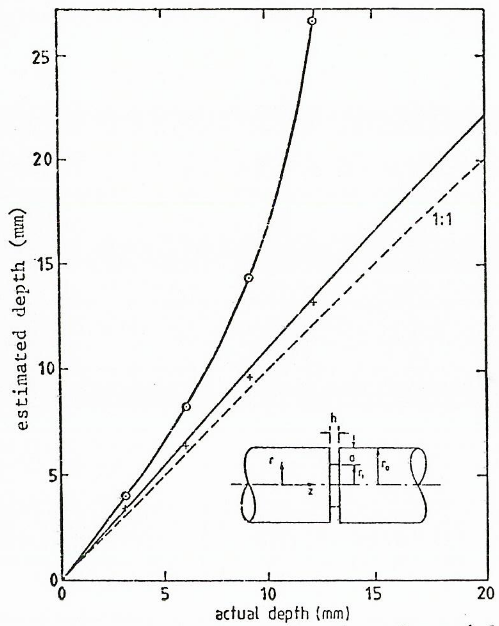

Fig 8. Experimental results for a circumferential groove in steel bar (37mm dia)
ʘ Eq. 2 + Ref. 2.